

Flow-distributed oscillations: Stationary chemical waves in a reacting flow

Mads Kærn and Michael Menzinger

Department of Chemistry, University of Toronto, 80 St. George Street, Toronto, Ontario, Canada M5S 1A1

(Received 27 May 1999)

A recent prediction of stationary waves in open, reacting flows is experimentally verified. We show that stationary waves are generated by a mechanism whereby the flow carries a time-oscillating subelement, behaving like a batch reactor, through space while a fixed boundary condition at the inflow locks the phase of the oscillation. This mechanism can generate stationary patterns when all diffusion coefficients are equal. The experimental system is the ferroin-catalyzed Belousov-Zhabotinsky reaction in a tubular reactor, fed by the outflow of a continuous flow stirred tank reactor (CSTR). Parameter conditions are such that the concentrations are constant in the CSTR while they oscillate in the flow tube. [S1063-651X(99)50910-0]

PACS number(s): 82.20.-w, 05.45.-a, 47.70.-n

I. INTRODUCTION

Andrésen *et al.* [1] have recently predicted theoretically that stationary chemical waves can form in a reactive flow of an activator-inhibitor system with equal diffusion coefficients. This is in contrast to the Turing mechanism where fast inhibitor diffusion is required for the formation of space-periodic structures. It appears surprising that stationary, space-periodic structures should develop at all in an open flow.

A reacting advection-diffusion system with equal diffusion and flow rates (“plug flow”) can, in one spatial domain, be described by

$$(\partial_t + v\partial_x)\mathbf{u} = F(\mathbf{u}) + D\partial_{xx}^2\mathbf{u}, \quad (1)$$

where $F(\mathbf{u})$ describes the kinetics of $\mathbf{u} = (u_1, u_2, \dots)$, D is the diffusion coefficient, and v the linear flow rate. The equal diffusion coefficients and flow rates exclude the Turing [2] and differential flow (DIFI) instabilities [3]. It is assumed that the system shows autonomous oscillations with period T under homogeneous conditions in the absence of a flow. This underlying Hopf mode is essential for the generation of a space-periodic structure in the presence of a flow.

The flow introduces a linear dependence between time and space. A volume-element initiated at the upstream boundary of the flow $x=0$ at $t=0$ will, in the presence of a plug flow, be located at $x=vt$ after time t . When the contribution from diffusion is negligible, the phase of an autonomously oscillating reaction within the volume-element will recur at equidistant spatial points. The wavelength of this space-periodic wave will be linear in flow rate and be given by

$$\lambda = vT. \quad (2)$$

Furthermore, the wave generated by this flow distributed oscillator (FDO) will be stationary if the value of the phase remains fixed at the inflow boundary [1].

Andrésen *et al.* [1] note that Marek and Svobodová [4] may have observed the stationary FDO wave as early as 1975. The experimental data, however, extend over less than a full wavelength and do not represent a space-periodic

wave. More importantly, the location of the wave front did not change when the flow rate was changed by a factor of 3 (Ref. [4], Fig. 16). It is therefore unlikely that the wave front originates from the FDO mechanism discussed here.

Experimentally we realize an appropriate boundary condition by feeding the flow tube with the outflow from a continuous-flow stirred tank reactor (CSTR). The unstable stationary state of a chemical batch oscillator can be stabilized by choosing a sufficiently high inverse residence time in the CSTR. This is illustrated in the bifurcation diagram (Fig. 1) of the three-variable Rovinsky-Zhabotinsky (RZ) model [5] with appropriate flow terms added. In the absence of a flow, the RZ model oscillates between the red and blue phases in Fig. 1. At a sufficiently high inverse residence time the stationary state becomes stable through a subcritical Hopf bifurcation. This stationary CSTR-output serves as the inflow to the tubular reactor where dynamics changes to that of a batch reactor (inverse residence time = 0.0 s^{-1}).

We confirm that stationary waves may form spontaneously in an open flow and that the wavelength increases linearly with the flow rate. The stationary wavelength is, however, significantly shorter than that predicted from Eq. (2).

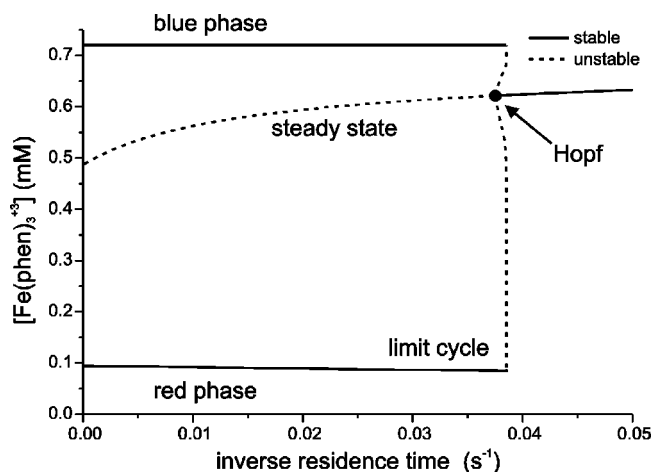


FIG. 1. Bifurcation diagram of the RZ model in a CSTR (see text). Parameters are $A=0.2 \text{ M}$, $B=0.4 \text{ M}$, $H=0.15 \text{ M}$, $C=7.5 \times 10^{-4} \text{ M}$. The stationary states and the oscillation amplitude are shown.

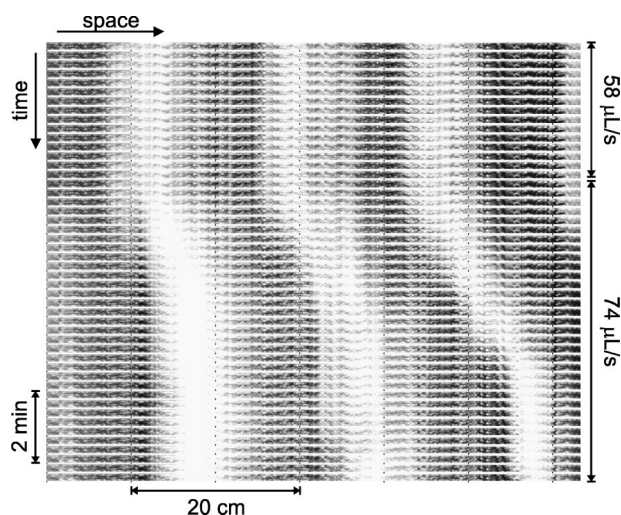


FIG. 2. Transition between stationary waves induced by a change in the flow rate. White corresponds to high ferriin.

We show numerically that diffusion can account for the shortening of the wavelength. Finally, we underline the importance of spatially uniform flow rate (plug flow) by comparing with an experiment with a parabolic flow profile (Poiseuille flow).

II. EXPERIMENTS

Two versions of the experiment were done. Experiment A (plug flow) employed a 10 mm (inner diameter) glass tube that was filled with 3 mm glass beads to create a plug flow profile. The volume fraction occupied by the beads was measured to be 67%, corresponding to a free volume of 0.26 mL/cm. In experiment B the glass tube (5 mm ID) was left empty and the flow profile was parabolic. The tube(s) were placed vertically on a back-lit milk-glass plate and were monitored using a charged-coupled-device camera mounted with a 450–550 nm bandpass filter.

The tubular reactor(s) were fed by the outflow of a 4.5 mL glass CSTR and the volumetric flow rate of the reactants served as the control parameter. The concentrations in the feedstream were $[\text{ferriin}] = 7.5 \times 10^{-4}$ M, $[\text{malonic acid}] = 0.4$ M, $[\text{bromate}] = 0.2$ M, and $[\text{sulfuric acid}] = 0.15$ M. The CSTR was monitored by a Pt-electrode connected to a double junction Ag/AgCl-electrode, placed in the premixed feedstream prior to the CSTR.

III. RESULTS

Figure 2 shows two stationary, space-periodic FDO waves observed under plug-flow conditions and the relaxation from one stationary wave to another brought about by a change of volumetric flow rate from $58 \mu\text{L/s}$ (top) to $74 \mu\text{L/s}$ (bottom). These volumetric flow rates correspond to linear flow rates of 13 and 17 cm/min, respectively. Each horizontal line is a snapshot of the tube taken 15 sec apart. The top 14 frames of Fig. 2 were obtained at the lower flow rate and the remaining frames at the higher flow rate. The wavelength of the stationary wave is 17 ± 1 cm in the top frame which relaxes to 20 ± 1 cm in the bottom frame. The downstream and the upstream edges of the stationary waves are fuzzy and

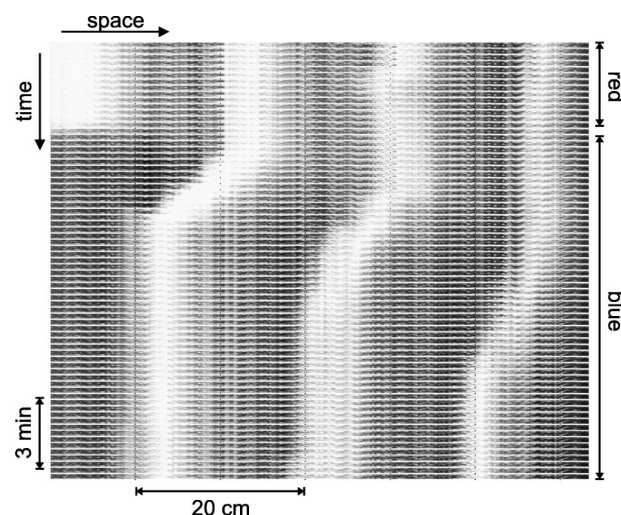


FIG. 3. Transition between stationary waves with identical wavelengths (see text).

the optical density is nonuniform even within a wave front (white segments in Fig. 2). The stationary waves are nevertheless stable but the wavelength can only be determined approximately. The wavelength was estimated from an average optical density profile obtained by averaging pixels at identical spatial distances followed by a nearest neighbor averaging.

The effect of changing the state of the CSTR is illustrated in Fig. 3. The CSTR was initially prepared in a quasi-stationary red state (top). This state was metastable under the conditions of the experiment and a sharp transition to the blue state occurred 24 min after the experiment was initiated. While the CSTR was in the red state four blue bands were visible. After the transition to the blue state the leftmost bands disappears and the remaining bands shift towards the inflow. After a rather long transient a new stationary wave is established. The stationary wavelengths corresponding to the different boundary conditions were measured in the frames located at the top and bottom of Fig. 3, respectively, and the change in initial condition does not change the wavelength significantly.

The dependence of the stationary wavelength on volumet-

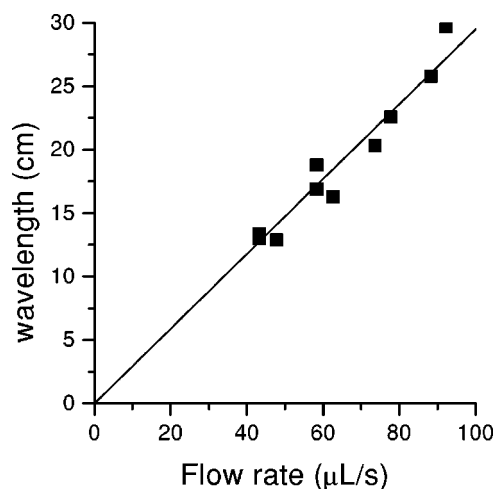


FIG. 4. Measured wavelength as function of flow rate.

ric flow rate is shown in Fig. 4. At flow rates below $43 \mu\text{L/s}$ the residence time is below the critical residence time and the CSTR oscillates. In this case traveling waves were observed. The slope of the linear fit to the experimental points in Fig. 4 is $0.30 \text{ cm s}/\mu\text{L}$, corresponding to an apparent batch period of 78 s [Eq. 2]. This value is 40% shorter than the measured batch oscillation period of $T \sim 130 \text{ s}$.

We note that Eq. (2) was obtained from Eq. (1), neglecting diffusion. Among the possible sources of the discrepancy between the actual and calculated period we were able to eliminate the effects of CO_2 accumulation, oxygen interference, and mixing effects in the CSTR. We were led to the conclusion that turbulent diffusion in the packed bed may account for the decreased wavelength. In a packed bed the effective diffusion rate is significantly higher than molecular diffusion [6] due to the turbulent hydrodynamics. The fuzzy but smooth edges of the stationary waves in Fig. 2 and 3 are an indication of significant diffusion since the batch oscillation has a sharp, autocatalytic ignition followed by a smooth decay into the red phase. A similar sharp leading wave front is expected in the tube in the absence of diffusion. The molecular mechanism responsible for the oscillation shape is well understood [7]. The inhibitor (bromide) is only generated in significant amounts during the blue phase of the oscillation. The inhibitor and the activator (HBrO_2) react and deplete each other and the high concentration of inhibitor produced during the blue phase slowly brings the system into the red phase. When the inhibitor is depleted below a critical concentration the activator ignites and the system re-enters the blue phase. In the presence of diffusion, the activator will diffuse from the sharp ignition front into the tail of the preceding red phase. This increased activator concentration in the red phase increases the rate of inhibitor depletion, hence, the system reaches the critical inhibitor concentration faster than it would in the absence of diffusion.

Figure 5 demonstrates the effect of diffusion in the RZ model. Panel A illustrates the behavior in a pure reaction-advection system, whereas the panel B is obtained by a numerical simulation with a high effective diffusion coefficient. The effective diffusion coefficient D_e in a packed bed may be estimated to be $D_e = d_p v$, where d_p is the diameter of the spherical packing material [6,8]. Based on this estimate the effective diffusion coefficient is $5.1 \text{ cm}^2/\text{min}$ ($d_p = 0.3 \text{ cm}$), hence, the magnitude of the diffusion coefficient $D = 4.7 \text{ cm}^2/\text{min}$ (see Fig 5) used in the numerical simulation is reasonable.

The simulations in Fig. 5 were initiated with spatially uniform initial concentrations equal to those in the CSTR with an inverse residence time of 0.04 s^{-1} . This CSTR output was also used as inflow to the tube. The top of the simulations show that the initial state oscillates in the absence of a flow. The Hopf mode is, however, pushed out of the tube when the flow is turned on (at $t=0$) and is replaced by a space-periodic wave. In the pure reaction-advection system (a) the transition between the time-periodic and the space-periodic mode is instantaneous at the boundary between subvolumes originating from the spatially homogeneous initial state and those carried by the flow. The space-periodic wave eventually fills the tube with a wavelength determined by Eq. (2). When diffusion is included (b), the transition between the Hopf mode and the space-periodic mode becomes

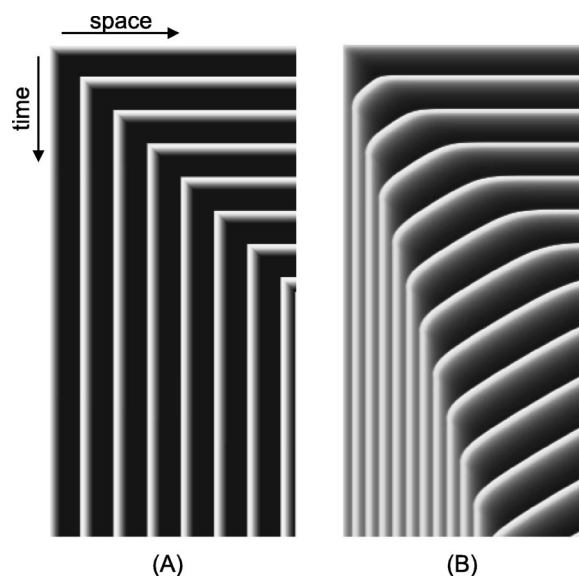


FIG. 5. Role of diffusion in numerical simulations. The tube was initially filled uniformly and the horizontal stripes are the resulting synchronous oscillations. This Hopf-mode is pushed out by the flow and replaced by a space-periodic wave. The width of the systems is $200\Delta x$ and the total integration time 400 s . The linear flow rate was set to $v = \Delta x \text{ s}^{-1}$, which gives the same resolution for space and time. Panel A illustrates the stationary wavelength in the absence of diffusion, whereas the diffusion coefficient in panel B was $D = \Delta x^2 \text{ s}^{-1}$. With the spatial scale $\Delta x = 0.28 \text{ cm}$, the linear flow rate is to $v = 17 \text{ cm}/\text{min}$. and $D = 4.7 \text{ cm}^2/\text{min}$, corresponding to the experimental range (see text).

smooth and the relaxation time to the stationary wave front becomes longer for each successive front. Similar behavior was observed in Figs. 2 and 3 in response to increased flow rate and changed boundary condition. In fact, the shape of the relaxation observed in Fig. 5 closely resembles what was observed experimentally when the empty tube was initially filled (not shown). Finally, the wavelength of the stationary wave is in the presence of diffusion reduced by 60% relative to the wavelength in the pure reaction-advection system. We conclude that turbulent diffusion accounts well for the 40% decrease in wavelength observed experimentally.

In experiment B we used an empty flow tube in which the velocity profile is known to be parabolic (Poiseuille flow). Since the wavelength is linear in the flow rate the presence of a laminar flow will make the wavelength depend on radial position. When diffusion is negligible, the wavelength is given by

$$\lambda(r) = v_0 \left[1 - \left(\frac{r}{r_0} \right)^2 \right] T, \quad (3)$$

where v_0 is the centerline flow rate, $r < r_0$ is the distance from the center of the tube, and r_0 is the tube radius. Figure 6(a) shows a snapshot of the first wave front closest to the inflow. This was the only detectable wave front. Figure 6(b) illustrates the radial profile of the oscillation front as predicted by Eq. (3). Each line in (b) corresponds to sequential equidistant phase values when the phase is radially homogeneous at the left edge. The distortion of the wave front by

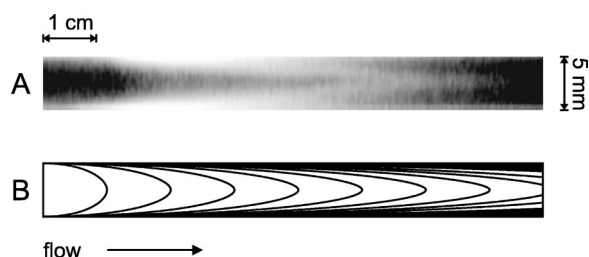


FIG. 6. Effect of a parabolic flow profile. (a) Actual experiment, (b) distortion of the phase due to Poiseuille flow.

Poiseuille flow combined with dephasing through diffusion prevents observation of the FDO wave in this case.

IV. CONCLUSION

We have demonstrated experimentally that stationary space-periodic waves can form through flow-distributed oscillations (FDO) in a reactive flow where all species have similar transport properties. These waves were predicted

theoretically in Ref. [1] but their physical interpretation was somewhat obscured by the emphasis on mathematical formalism. It turns out that the stationary waves are generated by a very simple, kinematic mechanism: a batch-mode oscillator is spatially resolved in the presence of a uniform flow. If the phase of the oscillation is fixed at the inflow, the oscillation phase will be locked in space and a stationary wave will emerge. In fact, any boundary condition with constant concentrations located within the basin of attraction of the batch mode limit cycle will generate a stationary spatial wave in the presence of a flow.

Our results support this simple interpretation. The stationary wavelength is independent of the boundary condition as long as the inflow concentrations remain constant. The wavelength of the stationary wave is directly proportional to the flow rate. This is consistent with a time oscillating subelement being carried through space by the flow. The stationary wavelength is, however, significantly shorter than the predicted wavelength, which may be accounted for by a high rate of turbulent diffusion. We are currently in the process of testing this hypothesis.

-
- [1] P. Andréßen, M. Bache, E. Mosekilde, G. Dewel, and P. Borckmans, *Phys. Rev. E* **60**, 297 (1999).
- [2] A.M. Turing, *Philos. Trans. R. Soc. London, Ser. B* **327**, 37 (1952).
- [3] A.B. Rovinsky and M. Menzinger, *Phys. Rev. Lett.* **70**, 778 (1993).
- [4] M. Marek and E. Svobodová, *Biophys. Chem.* **3**, 263 (1975).
- [5] A.M. Zhabotinsky and A.B. Rovinsky, *J. Phys. Chem.* **94**, 8001 (1990).
- [6] G. F. Froment and K. B. Bischoff, *Chemical Reactor Analysis and Design*, Wiley Series in Chemical Engineering (Wiley, New York, 1990).
- [7] R. J. Field and M. Burger, *Oscillations and Traveling Waves in Chemical Systems* (Wiley, New York, 1985).
- [8] V. Z. Yakhnin and M. Menzinger, *Chem. Eng. Sci.* **54**, 4547 (1999).